Particle Control under Wall Saturation in Long-pulse High-density H-mode Plasmas of JT-60U

H. Kubo, T. Nakano, N. Asakura, H. Takenaga, K. Tsuzuki, N. Oyama, H. Kawashima, K. Shimizu, H. Urano, K. Fujimoto, the JT-60 team

Japan Atomic Energy Agency, Naka, Ibaraki-ken, 311-0193 Japan

e-mail contact of main author: kubo.hirotaka@jaea.go.jp

Abstract. Long-pulse high-density H-mode plasmas have been sustained by divertor pumping under global wall saturation. The energy confinement and ELM activity can be sustained, while wall pumping does not work and even outgas appears. The outgas is attributed to increase in the divertor-plate temperature. On the other hand, wall pumping continues for longer than 20 s in high-density discharges with an X-point MARFE and detached divertor plasma. The X-point MARFE has also been controlled by the divertor pumping. Although the density control by the divertor pumping and the gas puffing is effective under the wall saturation, the wall-pumping rate changes to maintain the electron density against the electron density control. The change in the wall pumping suggests dynamic equilibrium between particle flux and desorption as an important wall-pumping mechanism.

1. Introduction

Particle control is one of the key issues for steady-state operation. In short discharges, the first wall absorbs hydrogen particles and it works as a pump (wall pumping). The wall pumping is effective to control the plasma density. However, in future tokamak devices, wall retention increases in a long discharge. Then, it is expected that the wall retention is saturated and the wall pumping does not work. Therefore, for steady-state operation, particle control by active divertor pumping without the wall pumping should be established. On the other hand, tritium retention in the wall is a crucial issue for safety in fusion devices. Understanding the wall-pumping mechanism is necessary for the particle control. In TRIAM-1M [1] and Tore-Supra [2], particle control and wall pumping in long-pulse discharges have been studied for limiter configurations. However, study of particle control using divertor pumping and wall-pumping mechanisms in long-pulse H-mode plasmas is still a significant topic to be explored [3]. In JT-60U, long-pulse operation up to 65 s with NBI of ~12 MW for 30 s has become available since 2003. Global saturation of the wall retention has been observed by repeating long-pulse high-density H-mode discharges [4-8]. In the experiments, difficulty of the density control under the wall saturation was shown [5].

In this paper, particle control and wall pumping under wall saturation in long-pulse high-density H-mode plasmas has been studied in JT-60U. The electron density has been controlled by the divertor pumping under the global wall saturation in H-mode plasmas. Mechanisms of the wall saturation are investigated. Change of the wall pumping with the density control is investigated in the long-pulse H-mode plasmas.

2. Experiment

JT-60U has a W-shaped divertor at the bottom. Inner and outer inclined divertor plates and a divertor dome in the private flux region form a W-shaped structure connecting to inner and outer baffle plates. Carbon fiber composite (CFC) materials are used for the divertor plates, the divertor dome top, and the outer wing of the divertor dome. Graphite materials are used for the inner wing of the divertor dome, the baffle plates, and most of the main chamber wall.

Ferritic steel plates are installed in upper outside areas of the main chamber to reduce the toroidal field ripple [9]. The area covered by the ferritic steel plates is ~10% of the surface of the vacuum-vessel. The baking temperature of the vacuum vessel is 150 or 300ºC during the experiment. For divertor pumping, toroidally continuous pumping slots are arranged between the inner and outer divertor plates and the divertor dome. The widths of the inner and outer pumping slots are 3 cm and 2 cm, respectively. Neutral particles entered the pumping slots are exhausted through under the outer baffle plates and three pumping ports. The maximum pumping speed is 26 m^3/s and 47 m^3/s at the vacuum-vessel temperatures of 150 and 300ºC, respectively [8]. We can change the pumping speed in ~0.7 s during a discharge using three valves installed at the pumping ports. The neutral particle pressure under the baffle plates is measured with a Penning gauge, and the divertor-pumping rate is calculated from the neutral particle pressure and the pumping speed. Deuterium gas was puffed from the top of the main chamber.

The global particle balance inside the vacuum vessel at a time, t, is expressed as

$$dN(t)/dt = \Gamma_{gas}(t) + \Gamma_{NBI}(t) - \Gamma_{div}(t) - \Gamma_{wall}(t) \qquad (1).$$

Here, N(t), $\Gamma_{gas}(t)$, $\Gamma_{NBI}(t)$, $\Gamma_{div}(t)$, $\Gamma_{wall}(t)$ indicate the total number of deuterium ion and neutral atom in the vacuum vessel, the gas-puffing rate, the particle-fueling rate of NBI, the divertor-pumping rate, and the wall-pumping rate, respectively. When Γ_{wall} is zero, the wall is globally saturated. The globally saturated means that all area of the wall is not necessarily saturated and it is possible that some of the area is releasing particles while the other areas are still pumping. When Γ_{wall} is positive, the wall pumping is active as a whole. When Γ_{wall} is negative, outgas appears.

In the present experiment, long-pulse (~30 s) high-density (> 0.5 $n_{GW,}$ where n_{GW} is the Greenwald density) H-mode plasmas have been repeated to study particle behavior. The plasma current was 1.2 MA, the toroidal field was 2.3 T, the plasma volume was ~74 m^3, the n_{GW} was ~4.5 x 10^{19} m^{-3}. To obtain a high divertor-pumping rate, the separatrix strike points were set close to the divertor pumping slots. The typical distance between the separatrix and the pumping slot was ~3 cm and ~2 cm in the inner and outer divertors, respectively. The NBI power was 4-8 MW, and the NBI duration was < 30 s. In series repetition of the long-pulse high-density discharges, the electron density was usually controlled with a feedback technique by changing the gas-puffing rate. The gas-puffing rate to keep the electron density at a level was usually rather high in the first discharge of the series repetition, and the gas-puffing rate decreased gradually in the succeeding discharges. Some of the particles injected by the gas puffing and NBI were accumulated in a few discharges [4]. After several long-pulse high-density discharges were performed, the discharges to be investigated in the following were obtained.

3. Results and Discussion

3.1 Wall-pumping in Long-pulse H-mode Plasmas

Waveforms of a typical long-pulse H-mode discharge with an electron density of 0.64 n_{GW} are shown in FIG. 1. The electron density was controlled with a feedback technique by changing the gas-puffing rate. At the beginning, a large gas puffing was applied to reach the programmed electron density. After the electron density reached the programmed electron density, the gas-puffing rate gradually decreased in ~8 s to keep the electron density, and it

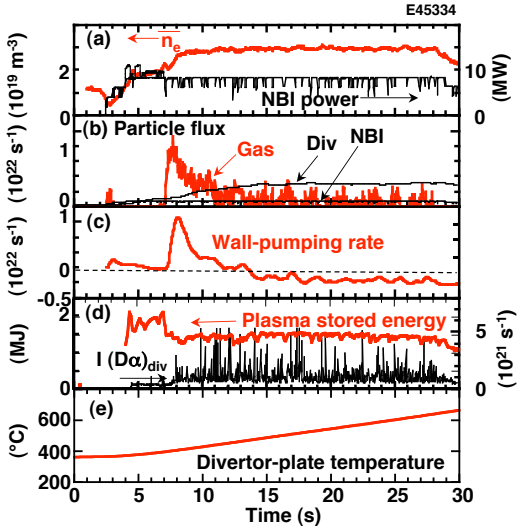

FIG.1. Waveforms of a long-pulse H-mode discharge with an electron density of 0.64 n_{GW}. (a) Line-averaged electron density and NBI power, (b) gas-puffing rate, particle-fueling rate of NBI, and divertor-pumping rate, (c) wall-pumping rate, (d) plasma stored energy and intensity of D_α emission from the divertor plasma, (e) divertor-plate temperature near the outer strike point. The vacuum-vessel temperature was 150ºC. The curves of the divertor-pumping rate and the wall-pumping rate were smoothed with a time constant of 200 ms.

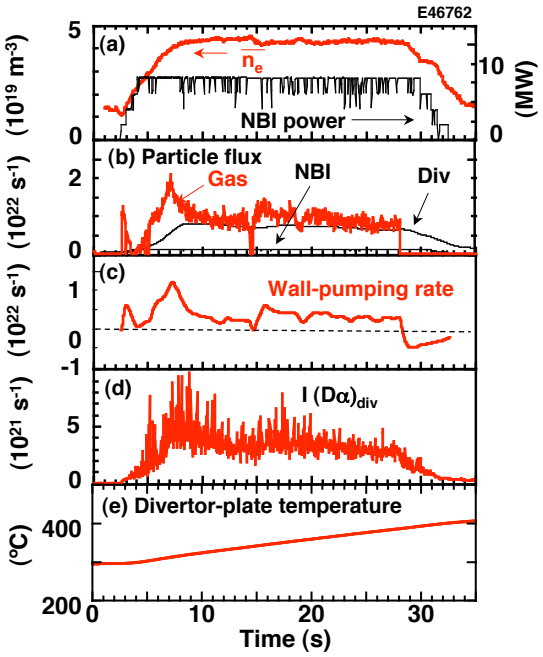

FIG.2. Waveforms of a long-pulse H-mode discharge with an electron density of 0.82 n_{GW}. (a) Line-averaged electron density and NBI power, (b) gas-puffing rate, particle-fueling rate of NBI, and divertor-pumping rate, (c) wall-pumping rate, (d) intensity of D_α emission from the divertor plasma, (e) divertor-plate temperature near the outer strike point. The vacuum-vessel temperature was 150ºC.

became almost constant. The wall-pumping rate was positive at the beginning, and it decreased to a negative constant in ~8 s. It shows that wall inventory was globally saturated and outgas appeared. As a result, under the global wall saturation, even with the outgas, the electron density was kept constant using the divertor pumping. Moreover, for ~20 s, the improved confinement and the ELM activity was sustained with the outgas (H_{89PL} ~ 1.3, $HH_{98(y,2)}$ ~ 0.71, where H_{89PL} is the ratio of the energy confinement time to the energy confinement time described by the ITER L-mode scaling and $HH_{98(y,2)}$ is the ratio of the thermal energy confinement time to the thermal energy confinement time described by IPB98(y,2) scaling.). Although the confinement improvement was not high, it was a usual level considering confinement degradation with the electron density in JT-60U [10]. In previous JT-60U experiments, it was difficult to control the electron density under the wall saturation [5]. The improvement was obtained by setting the separatrix strike points closer to the pumping slots and adjusting parameters for the feedback density control. In the bottom column of FIG. 1, time evolution of the maximum divertor-plate temperature is shown. The maximum temperature was measured near the outer strike point with a thermocouple mounted ~5 mm below the surface. The temperature of the outer divertor plates was always higher than the temperature of the inner divertor plates. The temperature increased from 360 to 670ºC during the discharge. Relation between the outgas and the divertor-plate temperature is discussed later.

FIG. 2 shows a long-pulse H-mode discharge with an electron density of 0.82 n_{GW}. The gas-puffing rate was kept at a rather high level to sustain the high electron density. The wall-pumping rate was positive even in the later phase of the NB heating. It shows that the wall

inventory was not globally saturated for ~20 s. The increase in the divertor-plate temperature was small (~110ºC), since an X-point MARFE appeared and the divertor plasma was detached. As discussed later, since the increase in the divertor-plate temperature was small, it is expected that the outgassing rate should be smaller compared with the discharges with the electron density of 0.64 n_{GW}. Nevertheless, continuous wall-pumping mechanisms such as co-deposition should exist.

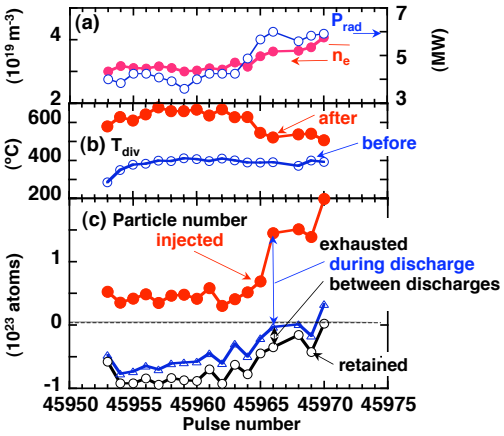

FIG. 3. (a) Line-averaged electron density, total radiation loss power, (b) divertor-plate temperature near the outer strike point before and after the discharges, (c) number of particles injected during the discharges, and change in the retained-particle number by the discharges at the end of the discharges and at the beginning of the next discharges in a series of long-pulse high-density H-mode discharges. In (c), the differences between the curves show the numbers of particles exhausted during the discharge and between the discharges. The NBI power was 8 MW, and the vacuum-vessel temperature was 300ºC.

FIG. 3 shows electron density, radiation loss power, divertor-plate temperature, number of particles injected during the discharges, and change in the number of the retained particles as a function of the pulse number for a series of long-pulse high-density H-mode discharges. In this series, after performing discharges with electron densities of ~0.65 n_{GW}, we performed discharges with higher electron densities up to ~0.8 n_{GW}. In the high-density discharges (#45965 - #45970), an X-point MARFE appeared and the radiation loss power was high. In these discharges, the divertor plasma was detached and increase in the divertor-plate temperature during the discharge was small. In these discharges, the divertor-pumping rate is high and the particle number injected during the discharge was high to keep the high density. For the low-density discharges, the change in the retained-particle number by the discharge at the end of the discharge was negative. It indicates that outgassing was dominant in these discharges. As the electron density increased, decrease in the retained-particle number became small. In the discharge with the electron density of ~0.8 n_{GW} (#45970), the change in the retained-particle number became positive. It indicates that the wall pumping was dominant in the high-density discharge. The number of particles exhausted between the discharges was smaller than that during the discharge. The wall inventory was decreased by repeating long-pulse H-mode discharges with electron densities of ~0.65 n_{GW}. The particle source for the decrease in the wall inventory seems to be the main chamber wall [8].

Here, we discuss mechanisms of the wall saturation and the wall pumping. The wall-pumping rate becomes almost constant in the later phase of the H-mode plasma (FIG. 1 and FIG. 2). The wall-pumping rate is plotted as a function of increase in the divertor-plate temperature in FIG. 4. As the NBI power increases, the temperature rise increases. As the electron density increases, the radiation loss power increases and the temperature rise decreases (FIG. 3). As shown in this figure, the wall-pumping rate decreases from positive to negative, as the rise in the divertor-plate temperature increases. In other words, the outgas tends to increase with the increase in the divertor-plate temperature. Difference between the 150ºC and 300ºC cases is due to difference in the outer strike point position; the distance between the outer strike point and the thermocouple in the 300ºC case was larger than that in the 150ºC case. In experiments of hydrogen implantation to carbon materials, saturation level of hydrogen inventory in

carbon materials decreases as the temperature of the carbon materials increases over ~100ºC [11]. Therefore, the outgas in the later phase of the H-mode plasma can be attributed to increase in the divertor-plate temperature.

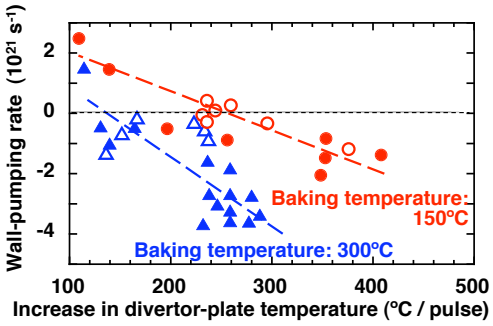

FIG. 4. Wall-pumping rate in the later phase of the H-mode plasma as a function of increase in the divertor-plate temperature near the outer strike point by the discharge. Open and solid symbols indicate the data obtained in discharges with an NBI power of 4 and 8 MW, respectively. The circles and triangles indicate the data at a vacuum-vessel temperature of 150 and 300ºC, respectively. The broken lines are to guide readers' eyes.

The positive wall-pumping rate observed at the later phase in high-density discharge (FIG. 2) indicates that continuous wall-pumping mechanisms such as co-deposition with carbon impurity should exist. In the discharge shown in FIG. 2, the total intensity of Dα emission from the divertor was ~3 x 10^{21} photons/s in the later phase. When we assume that the ratio of the deuterium ionization rate to the Dα emission rate is 18 [12] and the carbon-sputtering yield is 0.1 [13], the carbon impurity production rate is estimated to be ~5.4 x 10^{21} s^{-1}. Supposing all the produced carbon impurity made deposition layer with D/C = 0.05 measured in JT-60U [14], the deuterium co-deposition rate is estimated to be ~1 x 10^{20} s^{-1}. Compared with the observed wall-pumping rate of ~3 x 10^{21} s^{-1}, it seems difficult to account the wall-pumping rate by the co-deposition. Co-deposition rates estimated from intensity of CD band emission from the divertor was also too small to account the wall-pumping rate [8]. In Tore-Supra, continuous wall pumping has also been observed and it cannot be explained by co-deposition either [2]. In JT-60U, the wall-pumping rate seemed to increase with the particle flux to the wall. That is also discussed in the next section. Since this process can determine tritium retention in the vacuum vessel of the fusion reactor, further investigation is required to identify the wall-pumping mechanism.

3.2 Change of Wall Pumping with Density Control

The electron density control by the divertor pumping and the gas puffing is effective under the wall saturation, as described in the previous section. However, it is not straightforward to predict the density controllability, since the wall pumping changes with plasma-wall interaction. Change of the wall pumping with the density control has been investigated in the later phase where the wall-pumping rate becomes almost constant.

FIG. 5 shows a discharge in which the divertor pumping was off until 20 s and turned on at 20 s. When the divertor pumping was off, the electron density increased over the reference for the electron-density control without gas puffing only by NBI fuelling. As the electron density increased, the radiation loss power increased and an X-point MARFE appeared at 15 s. Then, the divertor plasma was detached, and the neutral particle pressure increased. After the divertor pumping was turned on at 20 s, the neutral particle pressure in the divertor and the electron density began to decrease and the MARFE disappeared. Since the intensity of the D_α emission decreased, the particle flux to the divertor area should be decreased. As a result, the divertor pumping successfully controlled the X-point MARFE. However, it should be noted that the outgas appeared when the divertor pump was on. When the divertor pumping was off, the particles fuelled by the NBI were almost absorbed by the wall. As described in the

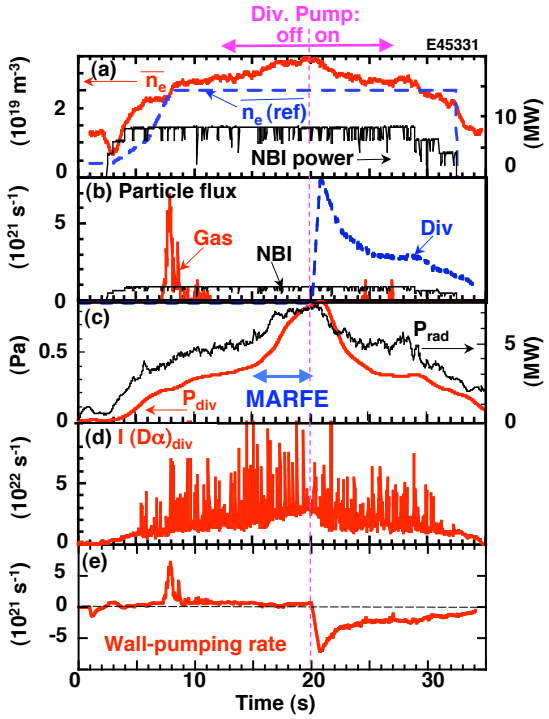

FIG. 5. Waveforms of a discharge in which the divertor pumping was turned on at 20 s. (a) Line-averaged electron density, reference for the electron density control, NBI power, (b) gas-puffing rate, particle-fueling rate of NBI, and divertor-pumping rate, (c) neutral particle pressure under the divertor baffle and total radiation loss power, (d) intensity of D_α emission from the divertor plasma, (e) wall-pumping rate. The vacuum-vessel temperature was 150ºC.

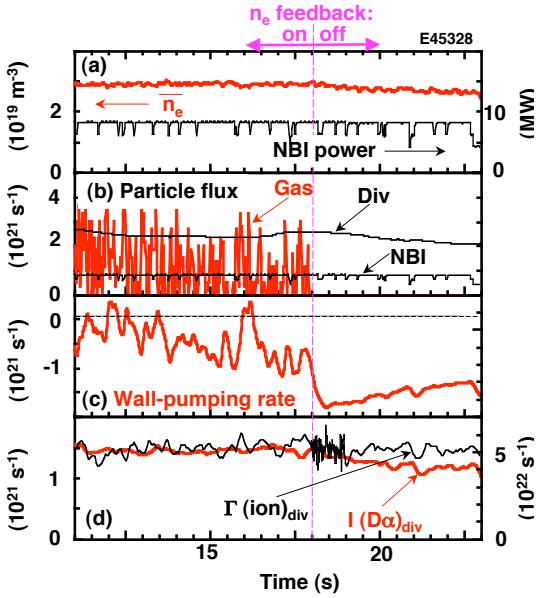

FIG. 6. Waveforms of a discharge in which the electron-density feedback control was turned off by gas-puff termination at 18 s. (a) Line-averaged electron density and NBI power, (b) gas-puffing rate, particle-fueling rate of NBI, and divertor-pumping rate, (c) wall-pumping rate, (d) intensity of D_α emission from the divertor plasma and total ion flux to the divertor plates. The curves of the Dα intensity and the ion flux were smoothed with a time constant of 200 ms. This discharge was an ELMy H-mode plasma, and the vacuum-vessel temperature was 150ºC.

previous section, the wall-pumping rate seemed to increase with the particle flux to the wall. However, in this discharge, while the electron density was decreasing after starting the divertor pumping, the wall-pumping rate was recovering after the drastic decrease. It suggests that a dynamic equilibrium between particle flux and desorption was established under high flux at high density [11,15], and the wall was releasing the retained particles in a few seconds as the particle flux decreased. By assuming the deuterium ionization rate to the Dα emission rate is 18, the decrease in the wall-pumping rate was ~0.02 of the decrease in the recycling flux.

FIG. 6 shows waveforms of a discharge in which the electron-density feedback control was turned off at 18 s by gas-puff termination. After the gas puff terminated, the electron density decreased gradually. It indicated that the density could be controlled by changing the gas-puffing rate. As the electron density decreased, the intensity of the Dα emission, the ion flux to the divertor and the divertor-pumping rate decreased gradually. However, the decrease in the divertor-pumping rate didn't exactly correspond to the decrease in the gas-puffing rate. Then, the wall-pumping rate became rapidly more negative as shown in the third column. In other words, outgas appeared with the gas-puff termination. This result also suggests that a dynamic equilibrium between particle flux and desorption was established under high flux and the wall was releasing the retained particles as the particle flux decreased. Outgas with gas-puff termination has also been suggested by analysis of electron-density decay time in

Tore Supra [16]. Calculation by a local mixing model showed outgas from the limier due to reduction in the particle flux by the gas-puff termination, and the calculation could simulate the time evolution of the electron density. In the local mixing model, the total concentration of hydrogen atoms is composed of mobile hydrogen (solute hydrogen) fraction and trapped one. The mobile-hydrogen concentration becomes high under high particle flux due to the equilibrium between the particle flux and the desorption, and the mobile hydrogen atoms are released when the particle flux decreases. On the other hand, enhancement of wall pumping by additional gas puff has been suggested from analysis of electron-density decay time in TRIAM-1M [17].

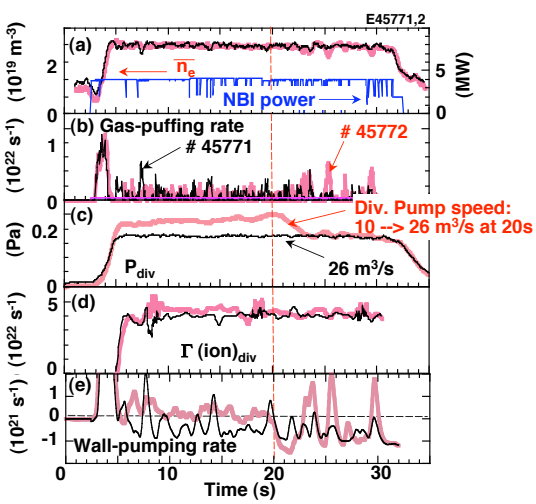

FIG. 7. Waveforms of a discharge in which the divertor-pumping speed was kept at 26 m^3/s (black and thin curve: #45771) and a discharge in which the divertor-pumping speed was changed from 10 to 26 m^3/s at 20 s (light and thick curve: #45772). (a) Line-averaged electron density and NBI power, (b) gas-puffing rate, (c) neutral particle pressure under the divertor baffle, (d) total ion flux to the divertor plates, (e) wall-pumping rate. These discharges were ELMy H-mode plasmas, and the vacuum-vessel temperature was 150°C.

In FIG. 7, a discharge in which the divertor-pumping speed was changed from 10 to 26 m^3/s at 20 s (#45772) is compared with a discharge in which the divertor pumping speed was kept at 26 m^3/s (#45771). In the discharge #45771, the three valves of the divertor pumping were open. In the discharge, the wall-pumping rate was a negative constant after ~ 7s. In the next discharge (#45772), only a valve was open and other two valves were closed before 20s, and all the three valves were opened after 20 s. The neutral particle pressure under the divertor baffle was decreased by increasing the divertor-pumping speed. By increasing the divertor-pumping speed, the wall-pumping rate changed from positive to negative at 20 s. Therefore, it indicates that outgas appeared after 20 s. By comparing the two discharges, before 20 s, the neutral particle pressure and the ion flux in the discharge with the pumping speed of 10 m^3/s was higher than those in the discharge with the pumping speed of 26 m^3/s. Then, the wall-pumping rate in the 10 m^3/s case was higher than that in the 26 m^3/s case. After 23 s, the neutral particle pressures, the ion flux, and the wall-pumping rates were similar in these discharges. Therefore, it suggested that the wall-pumping rate was high at high particle flux.

As a result, the density control by the divertor pumping and the gas puffing is effective. However, out gas appears when the electron density is controlled by increasing the divertor-pumping rate or by terminating the gas puffing. The experiment with changing the divertor pumping speed from 10 m^3 to 26 m^3 suggests that the wall-pumping rate increases with the particle flux. Therefore, the wall pumping tends to maintain the density against the density control. For design of divertor-pumping systems to control the electron density, a model that can simulate these phenomena should be established. Further investigation is needed for establishment of the model.

4. Summary

Particle control and wall pumping was studied under wall saturation in the long-pulse high-

density H-mode plasmas. The electron density was controlled by the divertor pumping in the long-pulse high-density H-mode plasmas where the wall pumping didn't work and even outgas appeared. The energy confinement and the ELM activity was sustained, while the outgas rate increased and the gas puff rate decreased. The X-point MARFE was also controlled by the divertor pumping. Therefore, the divertor pumping was effective to control the density. The outgas was attributed to increase in the divertor-plate temperature. Wall pumping continued for longer than 20 s in high-density discharges with an X-point MARFE and detached divertor plasma. The co-deposition with carbon impurity cannot account the continuous wall-pumping rate. The wall-pumping rate seemed to increase with the particle flux to the wall. Since this process can determine tritium retention in the vacuum vessel of the fusion reactor, further investigation is required to identify the wall-pumping mechanism. Although the density control by the divertor pumping and the gas puffing was effective, outgas appeared when the electron density is controlled by increasing the divertor-pumping rate or by terminating the gas puffing. It suggested dynamic equilibrium between particle flux and desorption. As a result, the wall pumping changed to maintain the electron density against the electron density control. For design of divertor-pumping systems to control the electron density, a model that can simulate these phenomena should be established. Further investigation is needed for establishment of the model.

Acknowledgements

The authors wish to thank Dr. M. Sugihara of Japan Atomic Energy Agency for providing useful information for this study. This work was partly supported by JSPS, Grant-in-Aid for Scientific Research (A) No. 16206093.

References

[1] SAKAMOTO, M., et al., Nucl. Fusion 42 (2004) 165.
[2] TSITRONE, E., et al., 2004 Proc. 20th Int. Conf. on Fusion Energy (Vilamoura, 2004) (Vienna: IAEA) CD-ROM file EX/10-2 and http://www-naweb.iaea.org/napc/physics/fec/fec2004/datasets/index.html.
[3] ASAKURA, N., Plasma Phys. Control. Fusion 46 (2004) B335.
[4] TAKENAGA, H., et al., J. Nucl. Mater. 337-339 (2005) 802.
[5] NAKANO, T., et al., Nucl. Fusion 46 (2006) 626.
[6] TAKENAGA, H., et al., Nucl. Fusion 46 (2006) S39.
[7] KUBO, H., the JT-60 team, Plasma Science & Technology 8 (2006) 50.
[8] NAKANO, T., et al., submitted to J. Nucl. Mater.
[9] SHINOHARA, K., et al., in this conference FT/P5-32.
[10] KUBO, H., et al., Nucl. Fusion 41 (2001) 227.
[11] MÖLLER, W. J., Appl. Phys. 64 (1988) 4860.
[12] JOHNSON, L. C., et al., J. Quant. Spectrosc. Radiat. Transfer 13 (1973) 333.
[13] ROTH, J., "Review and Status of Physical Sputtering and Chemical Erosion of Plasma Facing Materials", Nuclear Fusion Research (CLARK, R. E. H., REITER, D., Ed.), Springer, Berlin (2004) 203-224.
[14] TANABE, T., Fusion Eng. Des. 81 (2006) 139.
[15] MATSUHIRO, K., et al, 2000 Proc. 18th Int. Conf. on Fusion Energy (Sorrento, 2000) (Vienna: IAEA) CD-ROM file FTP1/22 and http://www.iaea.org/programmes/ripc/physics/fec2000/html/node1.htm.
[16] SUGIHARA, M., et al., J. Nucl. Mater. 266-269 (1999) 691.
[17] SAKAMOTO, M., et al., J. Nucl. Mater. 313-316 (2003) 519.